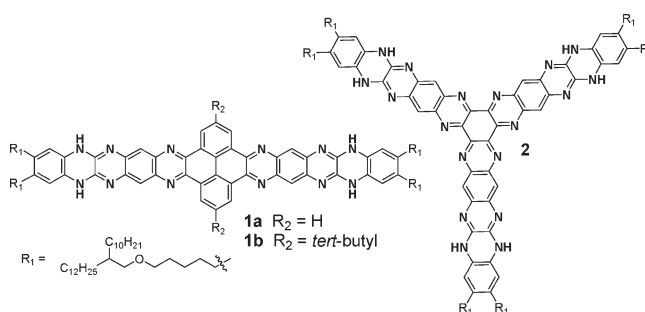


Large-Size Linear and Star-Shaped
Dihydropyrazine Fused PyrazinacenesChenhua Tong,[†] Wenguang Zhao,^{†,§} Jing Luo,^{†,||} Hongying Mao,[†] Wei Chen,^{†,‡}
Hardy Sze On Chan,^{*,†} and Chunyan Chi^{*,†}Department of Chemistry, National University of Singapore, 3 Science Drive 3,
Singapore, 117543, and Department of Physics, National University of Singapore,
2 Science Drive 3, Singapore, 117542

chmcs@nus.edu.sg (Chan); chmcc@nus.edu.sg (Chi)

Received November 17, 2011

ABSTRACT



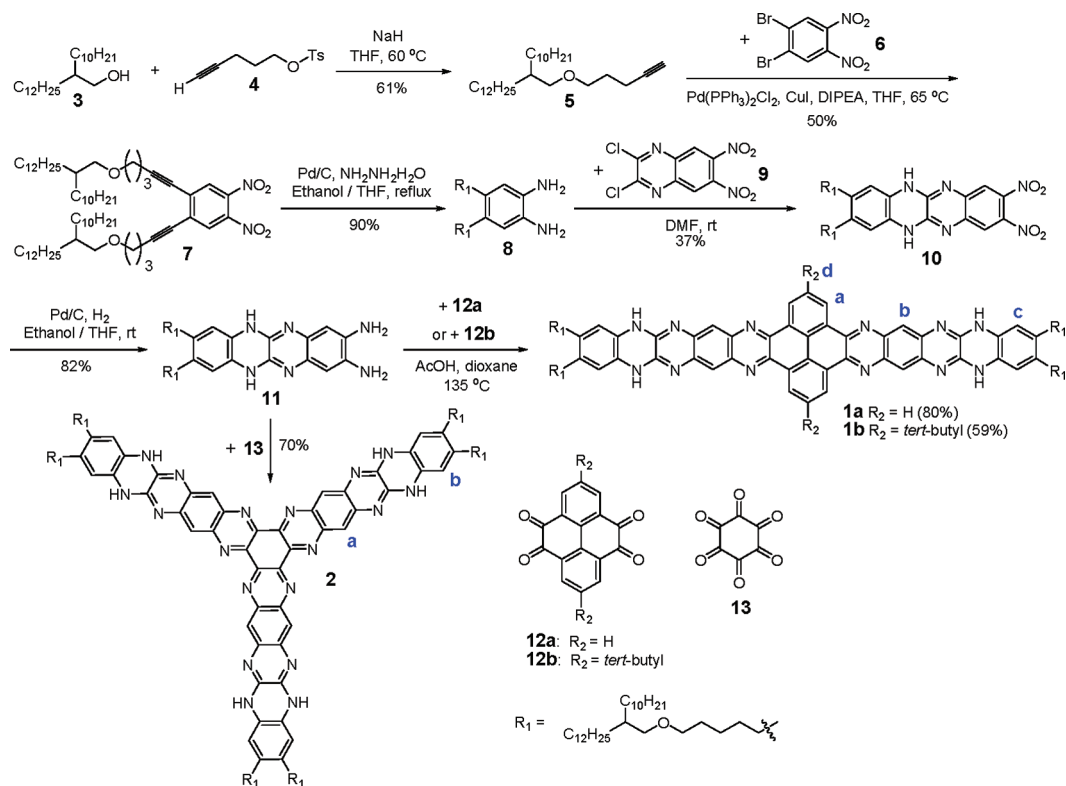
Linear and star-shaped pyrazinacenes **1a–b** and **2** were synthesized via condensation between a new building block **11** and pyrene tetraones or cyclohexaone. Compound **2** represents the largest star-shaped dihydropyrazine fused pyrazinacene reported so far. These largely expanded pyrazinacenes show good solubility and have a strong tendency to aggregate in both solution and thin films, indicating their potential applications for organic electronic devices.

Acene derivatives have attracted much attention because of their applications as semiconducting materials for organic electronic devices.¹ Long acenes are valuable in view of their large orbital area for stacking, ambipolar

property, and possible diradical property; however, they are usually unstable due to their high-lying HOMO energy level.² Peripheral substitution by electron-withdrawing carboxylic imide, cyano, or fluorine groups can stabilize the acenes and also offer n-type properties by lowering the

[†] Department of Chemistry.[‡] Department of Physics.[§] Present address: Institute of Chemical and Engineering Sciences, 1 Pesek Road, Jurong Island, Singapore 627833.^{||} Present address: School of Chemical and Material Engineering, Jiangnan University, Wuxi 214122, PR China.(1) (a) Bendikov, M.; Wudl, F.; Perepichka, D. F. *Chem. Rev.* **2004**, *104*, 4891. (b) Anthony, J. E. *Chem. Rev.* **2006**, *106*, 5028. (c) Anthony, J. E. *Angew. Chem., Int. Ed.* **2008**, *47*, 452.(2) (a) Anthony, J. E.; Facchetti, A.; Heeney, M.; Marder, S. R.; Zhan, X.-W. *Adv. Mater.* **2010**, *22*, 3876. (b) Bendikov, M.; Durrant, H. M.; Starkey, K.; Houk, K. N.; Carter, E. A.; Wudl, F. *J. Am. Chem. Soc.* **2004**, *126*, 7416.(3) (a) Sakamoto, Y.; Suzuki, T.; Kobayashi, M.; Gao, Y.; Fukai, Y.; Inoue, Y.; Tokito, S. *J. Am. Chem. Soc.* **2004**, *126*, 8138. (b) Swartz, C. R.; Parkin, S. R.; Bullock, J. E.; Anthony, J. E.; Mayer, A. C.; Malliaras, G. G. *Org. Lett.* **2005**, *7*, 3163. (c) Qu, H.; Cui, W.; Li, J.; Shao, J.; Chi, C. *Org. Lett.* **2011**, *13*, 924. (d) Katsuta, S.; Miyagi, D.; Yamada, H.; Okujima, T.; Mori, S.; Nakayama, K.; Uno, H. *Org. Lett.* **2011**, *13*, 1454.(4) (a) Maliakal, A.; Raghavachari, K.; Katz, H.; Chandross, E.; Siegrist, T. *Chem. Mater.* **2004**, *16*, 4980. (b) Chien, S.-H.; Cheng, M.-F.; Lau, K. C.; Li, W. K. *J. Phys. Chem. A* **2005**, *109*, 7509.(5) (a) Winkler, M.; Houk, K. N. *J. Am. Chem. Soc.* **2007**, *129*, 1805. (b) Ahmed, E.; Earmme, T.; Ren, G.; Jenekhe, S. A. *Chem. Mater.* **2010**, *22*, 5786–5796.(6) (a) Tonzola, C. J.; Alam, M. M.; Kaminsky, W.; Jenekhe, S. A. *J. Am. Chem. Soc.* **2003**, *125*, 13548. (b) Nishida, J.-I.; Naraso; Murai, S.; Fujiwara, E.; Tada, H.; Tomura, M.; Yamashita, Y. *Org. Lett.* **2004**, *6*, 2007. (c) Hu, J.; Zhang, D.; Jin, S.; Cheng, S. Z. D.; Harris, F. W. *Chem. Mater.* **2004**, *16*, 4912. (d) Lemaire, V.; da Silva Filho, D. A.; Coropceanu, V.; Lehmann, M.; Geerts, Y.; Piris, J.; Debije, M. G.; van de Craats, A. M.; Senthilkumar, K.; Siebbeles, L. D. A.; Warman, J. M.; Bredas, J.-L.; Cornil, G. *J. Am. Chem. Soc.* **2004**, *126*, 3271. (e) Jones, S. C.; Barlow, F.; Domercq, B.; Amy, F.; Kahn, A.; Brédas, J.-L.; Kippelen, B.; Marder, S. R. *J. Am. Chem. Soc.* **2005**, *127*, 16358. (f) Nishida, J.; Murakami, S.; Tada, H.; Yamashita, Y. *Chem. Lett.* **2006**, *35*, 1236. (g) Kojima, T.; Nishida, J.; Tokito, S.; Tada, H.; Yamashita, Y. *Chem. Commun.* **2007**, *14*, 1430. (h) Kaafarani, B. R.; Lucas, L. A.; Wex, B.; Jabbour, G. E. *Tetrahedron Lett.* **2007**, *48*, 5995. (i) Nakagawa, T.; Kumaki, D.; Nishida, J.; Tokito, S.; Yamashita, Y. *Chem. Mater.* **2008**, *20*, 2615. (j) Lee, D.-C.; Jang, K.; McGrath, K. K.; Uy, R.; Robins, K. A.; Hatchett, D. W. *Chem. Mater.* **2008**, *20*, 3688. (k) Lucas, L. A.; DeLongchamp, D. M.; Richter, L. J.; Kline, R. J.; Fischer, D. A.; Kaafarani, B. R.; Jabbour, G. E. *Chem. Mater.* **2008**, *20*, 5743.

Scheme 1. Synthetic Route of Pyrazinacene Derivatives **1a**, **1b**, and **2**



LUMO/HOMO energy level.³ An alternative strategy is to introduce N-atoms into an acene framework. The electronegative imine N-atoms can enhance the stability of acenes and prevent photooxidization and Diels–Alder reaction.⁴ Moreover, they can also serve as H-bond acceptors to increase the intermolecular interactions in the solid state.⁵

Owing to the high electron deficiency, imine N-atoms are usually utilized in the design of n-type semiconducting molecules.⁶ To achieve n-type behavior, a large number of imine N-atoms should be incorporated into the acene framework.⁵ Thus, pyrazine-containing acenes, namely, pyrazinacenes, are highly desired. Some linear pyrazinacenes have been reported.^{6,7} However, pyrazinacenes with high pyrazine unit density but without an electron-donating group can only be marginally obtained or they are very sensitive to even weak nucleophiles.⁸ Moreover, fused pyrazine derivatives are also readily reduced.⁹ On the other hand, a dihydropyrazine (reduced pyrazine) unit has been applied for the design of p-type semiconductors,¹⁰ and they

can also act as H-bond donors. Therefore, some aza-acene derivatives containing both imine and dihydropyrazine N-atoms have been prepared to adjust their stability and electronic properties.¹¹ An ambipolar behavior was expected for pyrazinacenes composed of both pyrazine and dihydropyrazine units.⁸ Besides the linear structures, star-shaped pyrazinacenes such as hexaazatriphenylene (HAT) and hexaazatrinaphthalene (HATN) derivatives are also of interest because they can self-organize into columnar structures in the solid state and allow one-dimensional charge transport along the column.¹² Larger linear and star-shaped acenes containing both pyrazine and dihydropyrazine units are interesting because they are supposed to show more extended π -conjugation and a higher tendency to aggregate, which are essential for material applications in electronic devices such as organic field-effect transistors (OFETs). However, synthesis of higher order (dihydro)pyrazinacenes is challenging because (1) the large rigid molecules usually show poor solubility if

(7) Gao, B.-X.; Wang, M.; Cheng, Y.-X.; Wang, L.-X.; Jing, X.-B.; Wang, F.-S. *J. Am. Chem. Soc.* **2008**, *130*, 8297.

(8) Richards, G. J.; Hill, J. P.; Subbaiyan, N. K.; D'Souza, F.; Karr, P. A.; Elsegood, M. R. J.; Teat, S. J.; Mori, T.; Ariga, K. *J. Org. Chem.* **2009**, *74*, 8914.

(9) Armand, J.; Boulares, L.; Bellec, C.; Pinson, J. *Can. J. Chem.* **1988**, *66*, 1500.

(10) (a) Miao, Q.; Nguyen, T.-Q.; Someya, T.; Blanchet, G. B.; Nuckolls, C. *J. Am. Chem. Soc.* **2003**, *125*, 10284. (b) Weng, S.-Z.; Shukla, P.; Kuo, M.-Y.; Chang, Y.-C.; Sheu, H.-S.; Chao, I.; Tao, Y.-T. *ACS Appl. Mater. Interfaces* **2009**, *1*, 2071.

(11) (a) Saso, H.; Takahashi, T. JP Patent 2004189674 A2 20040708, Jpn. Kokai Tokkyo Koho, 2004. (b) Stöcker, F.; Beckert, R.; Gleich, D.; Birkner, E.; Günther, W.; Görls, H.; Vaughan, G. *Eur. J. Org. Chem.* **2007**, 8, 1237.

(12) (a) Li, X. Y.; Tang, X. S.; He, F. C. *Chem. Phys.* **1999**, *248*, 137.
(b) Cornil, J.; Lemaire, V.; Calbert, J. P.; Brédas, J. L. *Adv. Mater.* **2002**, *14*, 726. (c) Ishi-i, T.; Hirayama, T.; Murakami, K.; Tashiro, H.; Thiemann, T.; Kubo, K.; Mori, A.; Yamasaki, S.; Akao, T.; Tsuboyama, A.; Mukaide, T.; Ueno, K.; Mataka, S. *Langmuir* **2005**, *21*, 1261.
(d) Ishi-i, T.; Murakami, K.; Imai, Y.; Mataka, S. *Org. Lett.* **2005**, *7*, 3175. (e) Ishi-i, T.; Yaguma, K.; Kuwahara, R.; Taguri, Y.; Mataka, S. *Org. Lett.* **2006**, *8*, 585.

not appropriately substituted by flexible alkyl chains; (2) there is no efficient way to extend the framework; and (3) the characterization of the strongly aggregated molecules is difficult. Herein, we report the successful synthesis and characterization of large-size linear aza-decacenes **1a–b** and star-shaped aza-tripentacene **2** containing both pyrazine and dihydropyrazine units. Their physical properties and self-assembly in solution and the solid state were also studied.

The synthesis of aza-acenes **1a–b** and **2** is shown in Scheme 1. The key intermediate compound is the alkylated dihydrotetraazatetracene 1,2-diamine **11**, which can undergo a condensation reaction with 1,2-diketones. To ensure sufficient solubility for the final products, branched dove-tail chains have to be attached onto the peripheries. The synthesis started from the etherification of 2-decytetradecan-1-ol **3** with pent-4-ynyl-4-methylbenzenesulfonate **4**¹³ to give the alkyne **5** in 61% yield. Hagihara–Sonogashira coupling between **5** and 1,2-dibromo-4,5-dinitrobenzene **6**¹⁴ gave compound **7** in 50% yield. It is worth noting that the spacer between an O-atom and a triple bond should be at least as long as propyl. Otherwise, a coupling reaction using alkynes with a shorter spacer (e.g., methylene) gave the corresponding products in extremely low yield, presumably due to the coordination of an O-atom to the Pd catalyst. Hydrogenation¹⁵ of both the nitro and the alkyne groups in compound **7** was then conducted by using hydrazine over Pd/C to afford the diamine **8** in 90% yield. The nucleophilic substitution/coupling reaction between **8** and **9**¹⁶ was highly energetic, and careful control must be exercised to achieve reasonable yield. The reaction can be conducted in solid form without solvent, but the purification was difficult because many byproducts were formed. After careful optimization of solvent and base, the reaction was found to show the best result when conducted in DMF without any base and **10** was obtained in 37% yield. Compound **10** was hydrogenated by hydrogen over Pd/C in ethanol and afforded the air-sensitive diamine **11**. The freshly prepared diamine **11** then reacted with pyrene tetraone **12a**, **12b**¹⁷ or cyclohexaone **13** to form the target products **1a**, **1b** and **2** in 59–80% yields. The *tert*-butyl-substituted pyrene tetraone **12b** was chosen as the bulk groups which may partially suppress molecular aggregation and facilitate NMR characterization in solution. These condensation reactions were carried out in acetic acid/*p*-dioxane at 135 °C, and excessive diamine **11** was used to ensure completion of multiple condensation reactions. The desired products

1a, **1b**, and **2** were nearly insoluble in alcohol and ethyl acetate but readily soluble in THF, aromatic solvents, chlorinated alkanes, and even hexane. During the reaction, the excessive diamine **11** formed the imidazole byproduct with acetic acid, which can be easily removed from the target products by simply washing with ethanol. Other condensation conditions such as *m*-cresol and *p*-toluenesulfonic acid/toluene were also tested, but the product was complicated. Further dehydrogenation of **1a**, **1b**, and **2** by oxidants such as MnO₂, PbO₂, or DDQ was also tried, but all of the reactions only gave partially dehydrogenated products which are difficult to purify and identify.

The chemical structures of **1a**, **1b**, and **2** were characterized by using NMR, MALDI-TOF mass spectrometry, and elemental analysis (see Supporting Information (SI)). Although they have very good solubility in chloroform or dichloromethane, no signal was observed in the aromatic region of NMR spectra even when the measurement was conducted at 100 °C in tetrachloroethane-*d*₄. Such a phenomenon can be attributed to the strong aggregation effect of the rigid core molecules in solution. TFA-*d*₁ was hence added to the solution to protonate the N-atoms to suppress the aggregation. As a result, a well resolved resonance signal was obtained and the chemical structures of **1a**, **1b**, and **2** were confirmed (Figure 1).

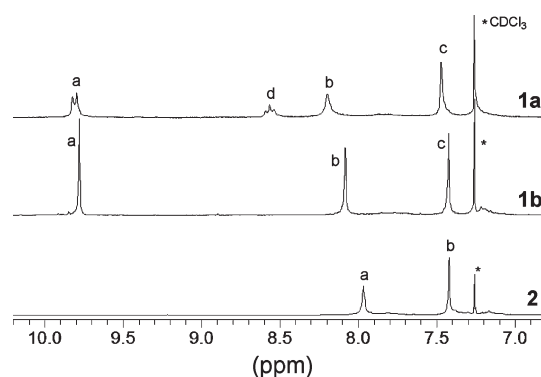


Figure 1. Aromatic regions of the ¹H NMR spectra of **1a**, **1b**, and **2** measured in CDCl₃/CF₃COOD (1:1). The resonances were assigned to the corresponding protons shown in Scheme 1.

The UV–vis absorption and fluorescence spectra of **1a**, **1b**, and **2** recorded in dilute chloroform solution and in a thin film are shown in Figure 2. **1a** shows an intense absorption band with a maximum at 506 nm at 1.0×10^{-5} M, and under the same conditions, **1b** exhibits two split bands at 500 and 524 nm (Figure 2a). For **1a**, the wavelength of the absorption maximum (λ_{\max}) also shows a slight hypsochromic shift with an increase of concentration (from 511 nm at 5×10^{-7} M to 505 nm at 3×10^{-5} M, Figure S1 in SI), which indicates a H-aggregation.¹⁸ For **1b**, because the aggregation is suppressed by the *tert*-butyl on the pyrene, no shift of λ_{\max} occurs at various concentrations and two resolved peaks were observed. Compound **2** displays a broad absorption band with

(13) Aucagne, V.; Berná, J.; Crowley, J. D.; Goldup, S. M.; Hänni, K. D.; Leigh, D. A.; Lusby, P. J.; Ronaldson, V. E.; Slawin, A. M. Z.; Viterisi, A.; Walker, D. B. *J. Am. Chem. Soc.* **2007**, *129*, 11950.

(14) Mørkved, E. H.; Neset, S. M.; Bjørlo, O.; Kjosen, H.; Hvistendahl, G.; Mo, F. *Acta Chem. Scand.* **1995**, *49*, 658.

(15) Zhang, F.; Bai, S.; Yap, G. P. A.; Tarwade, V.; Fox, J. M. *J. Am. Chem. Soc.* **2005**, *127*, 10590.

(16) Cai, S. X.; Kher, S. M.; Zhou, Z.-L.; Ilyin, V.; Espitia, S. A.; Tran, M.; Hawkinson, J. E.; Woodward, R. M.; Weber, E.; Keana, J. F. W. *J. Med. Chem.* **1997**, *40*, 730.

(17) (a) Hu, J.; Zhang, D.; Harris, F. W. *J. Org. Chem.* **2005**, *70*, 707. (b) Connor, D. M.; Allen, S. D.; Collard, D. M.; Liotta, C. L.; Schiraldi, D. A. *J. Org. Chem.* **1999**, *64*, 6888.

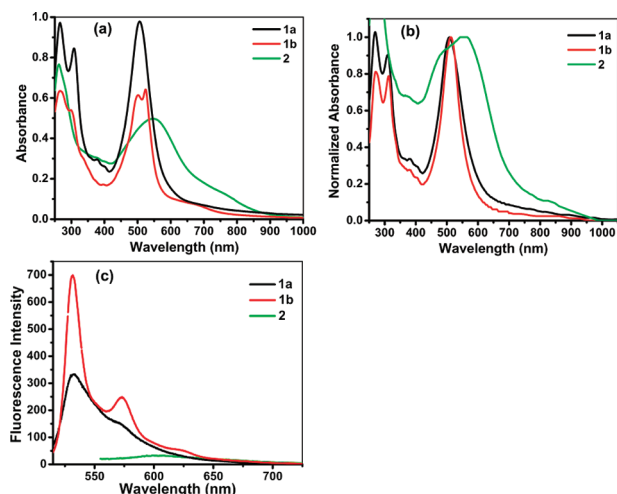


Figure 2. (a) UV–vis absorption spectra of **1a**, **1b**, and **2** in chloroform at 1×10^{-5} M. (b) Normalized UV–vis absorption spectra of **1a**, **1b**, and **2** in thin film. (c) Fluorescence spectra of **1a**, **1b**, and **2** in chloroform at 1×10^{-6} M.

λ_{max} at 547 nm in solution together with a long tail to the near-IR region (Figure 2a). The λ_{max} shows a red shift with increasing concentration (from 543 nm at 1×10^{-6} M to 558 nm at 5×10^{-5} M, Figure S1 in SI), which is similar to the HAT molecules and can be explained by a rotated cofacial aggregation.^{12c–e} In thin films, the absorption spectra of **1a** and **1b** become slightly broader and the spectrum of **2** shows an obvious red shift compared to that in solution (Figure 2b), indicating strong intermolecular association in film. Compound **1b** showed a relatively sharp fluorescence spectrum compared with **1a**, both with an emission maximum at 531 nm (Figure 2c). The fluorescence quantum yields are relatively low, with 3.5% for **1a** and 10.5% for **1b** (Rhodamine 6G as reference). Compound **2** exhibited very weak fluorescence (quantum yield < 0.5%) with an emission maximum at 601 nm. The concentration-dependent fluorescence spectra of **1a**, **1b**, and **2** (Figure S2 in SI) show a red shift of the emission maximum and fluorescence quench when the concentration is $> 1 \times 10^{-5}$ M. This further confirms the aggregates are formed in a concentrated solution ($> 1 \times 10^{-5}$ M).

Due to strong aggregation, the cyclic voltammetry measurements for **1a**, **1b**, and **2** were conducted in chlorobenzene at elevated temperature (80 °C), but only weak redox waves were obtained (Figure S3 in SI). Alternatively, ultraviolet photoelectron spectroscopy (UPS) was used to

Table 1. Energy Levels and Band Gaps of **1a**, **1b**, and **2**^a

	HOMO/eV	LUMO/eV	E_g^{opt} /eV
1a	−4.88	−2.79	2.09
1b	−5.04	−2.86	2.18
2	−4.90	−3.63	1.27

^a HOMO energy level was determined by UPS measurements in thin film state; E_g^{opt} is the energy band gap derived from the low-energy absorption edge in thin film state; LUMO = HOMO + E_g^{opt} .

determine their HOMO energy levels in thin films (Table 1, and Figure S4 and Table S2 in SI). The optical energy band gap (E_g^{opt}) was derived from the low-energy absorption edge in thin films, and then the LUMO energy level can be estimated by LUMO = HOMO + E_g^{opt} . Among these compounds, **2** has the lowest LUMO energy level due to the high pyrazine unit density.

The decomposition temperatures (T_d , corresponding to the 5% weight loss) for **1a**, **1b**, and **2** are at 300, 261, and 232 °C respectively (Figure S5 in SI). Differential scanning calorimetry (DSC) curves show no phase transition from rt to T_d (Figure S6 in SI). XRD patterns of thin films show one major reflection in the small angle region (with distances of 4.2, 3.27, and 3.53 nm for **1a**, **1b**, and **2**, respectively) and a halo at the wide angle region (4.1–4.6 Å) (Figure S7 in SI). The intensity of **1a** is much higher than the other two samples, implying that it has a higher packing order in the solid state.

In summary, large linear and star-shaped aza-acenes containing fused pyrazine/dihydropyrazine units were synthesized by using a new building block **11**. To the best of our knowledge, **2** represents the largest star-shaped dihydropyrazine fused pyrazinacene reported so far. These new molecules have a strong tendency to aggregate in both solution and thin films, and they might be used as good semiconductors for thin film OFETs. Device fabrication and characterization are underway in our laboratories.

Acknowledgment. This work is supported by the National University of Singapore under MOE AcRF FRC Grant R-143-000-444-112 and Start Up Grant R-143-000-486-133.

Supporting Information Available. Synthetic procedures and characterization data, additional UV–vis and fluorescence spectra, CV/UPS data, TGA/DSC curves, and XRD patterns. This material is available free of charge via the Internet at <http://pubs.acs.org>.

(18) Eisfeld, A.; Briggs, J. S. *Chem. Phys.* **2006**, 324, 376.